Preprint of paper submitted to Journal of Computational Acoustics, 1999

NONLINEAR INVERSION OF PIEZOELECTRICAL TRANSDUCER IMPEDANCE DATA

LAURA CARCIONE, JOHN MOULD, V. PEREYRA, D. POWELL, and G. WOJCIK

Weidlinger Associates, 4410 El Camino Real, Los Altos, California, U.S.A.

We describe a nonlinear least squares inversion algorithm for obtaining elastic and electromagnetic properties for piezoelectric materials from measured impedances. Richard Brent's PRAXIS, a general unconstrained minimization code is used for the nonlinear least squares fit. No explicit derivatives of the goal functional are required by this code. Bound constraints are imposed in order to limit the variability of the parameters to physically meaningful values. Since PRAXIS is an unconstrained optimization code, these constraints are introduced via a novel change of independent variables. The forward modeling is achieved by using a coupled finite element time domain code for the elastic and electro-magnetic parts of the problem. We also describe how a linearized sensitivity analysis can be used to suggest a priori which parameters can be calculated from impedances measured on a given sample. Numerical results are included.

1. Introduction

The problem we consider is that of inverting for the parameters describing a piezoelectric crystal model. Such a model is defined by elastic, electromagnetic, and coupling parameters, by the geometry of the sample and that of the electrodes

The objective of the nonlinear inversion process is to improve upon the accuracy of some nominal initial values of these parameters, using measured values at successive time intervals of the resulting impedance, when a small voltage is applied to the crystal.

We start this task with a complete set of forward modeling and optimization tools, namely PZFLEX and REVIEW [1], for the finite-element solution of the transient response of a piezoelectric material and for postprocessing the numerical results respectively. For the optimization part we use PRAXIS, an implementation of the Principal Axis method for the minimization of general functions [2].

The model we consider in this study requires ten parameters to describe the elastic and electromagnetic properties and the coupling between the two phenomenae. Current practice uses several IEEE standard shapes (corresponding essentially to asymptotic limit cases) in order to determine different groups of parameters at a time by trial and error.

As a preprocess, we propose to make sensitivity analyses of different crystal shapes, not necessarily in the IEEE set, in order to find configurations for which as many as possible

of the parameters can be determined. For this purpose we consider the linearized model, which is represented by the Jacobian matrix of first derivatives of the Fourier Transform of the impedance values with respect to model parameters. These derivatives are estimated by finite differences.

Since the number of parameters is small, we can apply a direct Singular Value Decomposition (SVD) based solver to this rectangular matrix calculated at a reference value of the parameters (in practice all these parameters are known within 10% of their true values, for a given material). As explained in [3], we can use the SV decomposition to rank the relative relevancy of each parameter, for a given data set. This can be used as a guide to design geometrical configurations and placement of electrodes so that the measured impedance is sensitive to as many parameters as possible, thus minimizing the number of samples that need to be built in order to determine material properties accurately.

To make this paper self-contained we will describe briefly the forward modeling algorithm; then we will explain how Jacobian matrices are calculated and describe the SVD based sensitivity estimation procedure. Finally we will present some numerical examples to show that this approach does work.

2. PZFLEX Modeling

Piezoelectric transducers convert electrical signals to mechanical signals and viceversa. They serve as transmitters and receivers in imaging systems for sonar, medical, and NDE (non-destructive evaluation) applications, as well as in nonimaging applications like SAW (surface acoustic wave) devices in signal processing.

One of the most technically demanding applications is ultrasound (ultrasonic) medical imaging. Operational emphasis for imaging transducers is broadband (impulsive) rather than narrowband (continuous wave). Transducers are currently available for diagnostic imaging and Doppler velocity measurement, as well as for a host of specialty applications (intracavity, biopsy, etc.) and disease treatment (lithotripsy, hyperthermia, tissue ablation). Over the last two decades the ultrasound industry has done a remarkable job in developing and refining these devices using a combination of semi-analytical design procedures and prototype experiments. However, it is apparent to many that conventional design methods are approaching practical limits of effectiveness. The industry has been slowly recognizing discrete numerical modeling on the computer as a complementary and useful solution.

Today nearly all of the major ultrasound system companies are experimenting with finite element models using commercial packages like ANSYS or by writing their own codes. Most have enjoyed only limited success at significant development and/or simulation costs. We suggest that the main source of difficulty is universal reliance on classical implicit algorithms for frequency-domain and time-domain analysis based on related experience with shock and wave propagation problems. In general, implicit algorithms are best suited to linear static problems, steady state vibrations, and low frequency dynamics. A much better choice for transient phenomena, linear or nonlinear, is an explicit time-domain algorithm which exploits the hyperbolic (wave) nature of the governing differential equations.

The finite element method reduces the electromechanical partial differential equations

(PDEs) over the model domain to a system of ordinary differential equations (ODEs) in time. This is done using one of the nearly equivalent integral formalisms: virtual work, weak form, Galerkin's method, weighted residuals, or less formally, using point-wise enforcement of the conservation and balance laws. The result is that spatial derivatives in the PDEs are reduced to a summation of "elemental" systems of linear algebraic equations on the unknown field values at nodes of the finite element discretization. The continuum elements used here are 4 node quadrilaterals in 2D and 8-node hexahedrons in 3D. The unknown field over an element is represented by low order shape functions determined by nodal (corner) values, i.e., bilinear in 2D and trilinear in 3D. Using a minimum of 15 elements per wavelength limits wave dispersion errors to less than 1%. Experience has shown these choices to offer the most robust basis for large-scale wave propagation analysis in structural and isotropic or anisotropic continuum models.

When transient signals are of principal interest, the most direct solution method is step-by-step integration in time. There are many ways to evaluate the current solution from known results at previous time steps. Implicit methods couple the current solution vector, hence, the global system of equations must be solved at each timestep. Their advantage is unconditional stability with respect to time step. By contrast, explicit methods decouple the current solution vector and eliminate the global system solve, but they are only conditionally stable, i.e., there is a time step limit (the Courant-Fiedrichs-Levy (CFL) condition) above which the method is unstable. The caveat for implicit integration of wave phenomena is that solution accuracy requires a time step smaller than one-tenth the period of the highest frequency to be resolved. This is close to the CFL stability limit for explicit methods and effectively removes the principal advantage of implicit integration.

Explicit integration of the field equations involves diagonalizing the uncoupled mass and damping matrices, using nodal lumping, replacing the time derivatives with finite differences, and integrating using a central difference scheme (2nd order accurate). For stability the time step must be smaller than the shortest wave transit time across any element (CFL condition). This follows from the hyperbolic (wave) nature of the original PDEs, i.e., during a time step the field at a point is only influenced by the field at neighboring points within a sphere of radius $\delta x = c_p \delta t$, where c_p is the fastest local wave speed. Therefore, for $\delta t \leq \delta x / c_p$, nodal fields are decoupled during a single time step and can be integrated independently.

An important issue in transducer modeling is frequency-dependent material damping. Regardless of the solution technique, fundamental assumptions must be made about the structure of the uncoupled damping matrices. The two most convenient damping models are mass-proportional and stiffness-proportional. A linear combination of the two is called Rayleigh damping. In the frequency-domain, coefficients are simply chosen to give the required damping at each calculated frequency. In the time-domain, constant coefficients yield damping that is inversely or directly proportional to frequency, or a linear combination. We also use a material-dependent, three-parameter viscoelastic damping model. Proper choice of viscosity constants and a relaxation time yields a damping maximum at the selected frequency and smooth fall-off. Therefore, viscoelastic models may be superposed to yield

a discrete spectrum of relaxation times that represent specified damping behavior over a limited frequency range, but at significant cost in memory.

The final issue is radiation boundary conditions. It is always necessary to truncate the finite element model in space because of limited computer memory. This is a fundamental problem in numerical simulation and requires special boundary conditions to reduce spurious reflections (grid truncation error). Time-domain continuum conditions are typically derived from the one-way wave equation, with an ad hoc approximation used to fit the discretization. Higher order implementations tend to degrade in 3D vector domains due to this ad hoc discretization. A new and better approach operates directly on the finite element equations using the general relation between spatial and temporal derivatives at an arbitrary wavefront. This yields boundary node velocity in terms of its derivatives over the element and stresses within the boundary element. The condition performs as well as a 4th order paraxial absorber, with lower computational overhead and less impact on stability.

More details, including validation, can be found in [4,5].

3. The Nonlinear Least Squares Problem

Given an homogeneous piezoelectric crystal, a small voltage is applied and the resulting impedance is calculated from measurements as a digitized function of time. This function is Fast Fourier Transformed and the resulting complex samples constitute the observed data, $\{I_i^o\}, i = 1, ..., m$.

Given a vector of model parameters $\boldsymbol{\alpha}$ and using the finite element simulator described above, we can calculate a similar response, that we call $\{I_i^c(\boldsymbol{\alpha})\}$.

The measured data will be subject to errors and if we assume that these errors are Gaussian distributed with zero mean this leads naturally to a least squares or best likelihood fit.

There is only a narrow range of the parameters that correspond to valid physically possible materials. If this feasibility range is not enforced the PZFLEX calculations may fail. Thus, calling $g(\boldsymbol{\alpha}) = \sum_{i=1}^{m}(I_i^o - I_i^c(\boldsymbol{\alpha}))^2$, the minimization problem we want to solve is:

$$\min_{\boldsymbol{\alpha}} g(\boldsymbol{\alpha}) \tag{3.1}$$

subject to:

$$\underline{\alpha}_i \leq \alpha_i \leq \bar{\alpha}_i$$

The bound constraints are used to limit the values of the model parameters to the physical relevant domain. These bound constraints can be handled in several ways:

1. Transformation into an unconstrained problem by using penalty functions;
2. Transformation into an unconstrained problem by using barrier functions;
3. Using standard constrained optimization algorithms.

Penalty and barrier functions are known to have severe limitations for this kind of problems, while techniques for constrained problems are considerably more complicated than

those for unconstrained ones. Besides, there is also a lack of reliable codes that are specialized to the nonlinear least squares problem.

Thus, we have chosen a different approach, which consists of a change of independent variables, so that when the new variables run over the whole space the physical parameters are constrained to the desired box. This can be achieved by using the transformation:

$$\alpha_i = \underline{\alpha}_i/(1+\exp x_i) + \bar{\alpha}_i/(1+\exp -x_i)$$

which has the desired properties. Thus, by starting at a feasible point we should always stay feasible. The inverse transformation is:

$$x_i = -\ln\left[(\bar{\alpha}_i - \alpha_i)/(\alpha_i - \underline{\alpha}_i)\right],$$

and those are the variables we will use in an unconstrained minimization algorithm to find the best fit of the data.

3.1. *Selecting Relevant Parameters Through the SVD Decomposition*

As a preliminary step it is of interest to consider several crystal samples with different geometries in order to find those that can lead to the determination of as many of the parameters as possible. This suggests a sensitivity analysis and it is necessary because the manufacturing of these samples is very costly and problematic.

Jupp and Vozoff [6] introduced the idea of relevant and irrelevant parameters, based on Singular Value Decomposition linearized analysis. We write first the Taylor expansion of the misfit vector around a given point $\boldsymbol{\alpha}$:

$$\mathbf{g}(\boldsymbol{\alpha}+\delta\boldsymbol{\alpha}) = \mathbf{g}(\boldsymbol{\alpha}) + \mathbf{J}(\boldsymbol{\alpha})\delta\boldsymbol{\alpha} + \mathbf{R}(\mathbf{g}, \delta\boldsymbol{\alpha}), \tag{3.2}$$

where $\mathbf{J}$ is the Jacobian of the goal functional $\mathbf{g}(\boldsymbol{\alpha})$ and $\mathbf{R}$ represents high order terms in the perturbation $\delta\boldsymbol{\alpha}$. In our problem, these partial derivatives are calculated by finite differences and thus require ten additional PZFLEX solves.

The Singular Value Decomposition of $\mathbf{J}$ can be written as:

$$\mathbf{J} = \mathbf{V}\mathbf{S}\mathbf{U}^{\mathbf{T}} = \sum_{i=1}^{r} s_i \mathbf{v_i} \mathbf{u_i^T}.$$

where $r \leq n$ is the rank of $\mathbf{J}$. The normalized singular values are defined as: $k_i = s_i/s_1$.

Introducing the *rotated parameters* (in tangent space):

$$\delta\mathbf{p} = s_1 \mathbf{V}^{\mathbf{T}} \delta\boldsymbol{\alpha},$$

and neglecting higher order terms, we can write (3.2) as:

$$\delta\mathbf{g} \approx \mathbf{J}\delta\boldsymbol{\alpha} = \sum_{i=1}^{r} k_i \delta p_i \mathbf{u_i},$$

which shows the direct relationship between the singular values and the rotated parameters, and also their influence on the variation of the misfit functional.
Thus,

$$\| \delta \mathbf{g} \|_2^2 = \sum_{i=1}^{r} k_i^2 \delta {p_i}^2,$$

since $\| \mathbf{u}_i \|_2 = 1$. This equation shows that the parameters δp_i that are associated with singular values that are small relative to s_1, will not contribute much to variations in the misfit functional.

That is the key to our algorithm for selecting the relevant parameter set.

1. Given a parameter vector $\boldsymbol{\alpha}$, calculate $\mathbf{J}(\boldsymbol{\alpha})$ and its SVD.
2. Let the matrix of the singular vectors scaled by the singular values be $\bar{\mathbf{V}}$.
3. Inspect the columns of $\bar{\mathbf{V}}$, and select the ones with l_2 norm above a certain threshold. Choose the indices of the variables in parameter space corresponding to these entries to form the subset IC of parameters that are most influenced by the data set.

4. Numerical Results

We consider a cylinder of piezoceramic material. The finite element modeling assumes two planes of symmetry: axial at half height and radial, in order to optimize the computation, which becomes 2D.

For a fixed diameter of 10 mm we consider several heights, giving aspect ratios (diameter/height) of 20/1, 5/1, 1/1, and 1/2. The 20/1 case corresponds to one of the IEEE standard shapes.

4.1. *Sensitivity Analysis*

By performing the analysis described in the previous section we have calculated the results shown in Table 1, where the numbers under the various parameters indicate how well determined they are when the real and imaginary part of the impedance are used as the data set. A value larger than 0.1 indicates a well determined parameter, while a value less than 0.01 indicates a poorly determined one. These numbers correspond to the Euclidean norms of the columns of the matrix V^T, scaled by the corresponding singular values.

These results indicate that considering truly three-dimensional shapes (such as the 1/1 or 1/2 aspect ratios), provides a better way to estimate more of the relevant parameters at once than the IEEE shapes. Of course, this is made possible because we can use PZFLEX to calculate the response of such a model. This is not possible with conventional asymptotic methods.

4.2. *Parameter Determination*

Table 1: Sensitivity analysis.

Aspect ratio	ep11	ep33	s11	s12	s13	s33	s44	d15	d13	d33
20/1	0.0006	0.62	0.79	0.2	0.04	0.07	0.0008	0.000003	0.51	0.07
5/1	0.07	0.3	0.89	0.25	0.07	0.07	0.01	0.01	0.58	0.04
1/1	0.05	0.5	0.4	0.12	0.3	0.44	0.075	0.087	0.41	0.66
1/2	0.046	0.42	0.4	0.12	0.21	0.56	0.086	0.083	0.26	0.74

We consider now the disk with aspect ratio 1/2 to test our parameter determination code. We will test PRAXIS, to least squares fit a data set consisting of the real and imaginary parts of the FFT of the impedance which, in the range $1KHz\ to\ 1MHz$ is represented in digital form by 1341 unequally spaced samples. One important feature of PRAXIS is that it does not require derivatives with respect to the unknown parameters.

Due to symmetries and the fact that the material is considered homogeneous, the problem can be cast as a 2D problem and for the wave lengths, materials and model size involved a mesh of 25×50 elements is appropriate. For a driving frequency of 3.75 MHz the elastic part of PZFLEX requires 7091 time steps. In a $300MHz$ Pentium II computer under the SOLARIS operating system an average solve takes approximately 75 seconds.

We first generate synthetic data by running PZFLEX with the set of parameters shown in Table 2 (the "target values"). Then we perturb these values by 5.0% and call them the "initial values". The objective is to see how many of the target values of these parameters we can recover, say to 1% accuracy or better, by using PZFLEX coupled with the unconstrained optimization code PRAXIS, in order to fit the synthetic data in the least squares sense. We also use the change of variables strategy explained above to force the parameters to stay within a $\pm 8\%$ box around the initial guess. After 172 evaluations (i.e., PZFLEX solves; a 3.5 hours job), PRAXIS produced the results shown in Table 3.

The begining and final residual mean squares were:

$$\begin{aligned} rms_0 &= 64844 \\ rms_{172} &= 1068 \end{aligned}$$

In Figures 1-4 we show the cross-plots of the target, and final, real and imaginary parts of the impedance spectrum for low and high frequencies separately. Observe that there is a change of scale, going from low to high frequency in order to enhance the details.

5. Solving the Optimization Problem Over the Internet

Table 2: Target parameters

Parameter	Value	Name
ep11	0.231e-7	dielectric constant
ep33	0.297e-7	dielectric constant
s11	1.559e-11	compliance term
s12	-0.441e-11	compliance term
s13	-0.819e-11	compliance term
s33	2.0e-11	compliance term
s44	4.48e-11	compliance term
d15	7.19e-10	piezoelectric stress constant
d13	-2.895e-10	piezoelectric stress constant
d33	6.0471e-10	piezoelectric stress constant

Table 3: Final parameters and errors

Parameter	Value	% error
ep11	0.231e-7	0.12
ep33	0.296e-7	-0.33
s11	1.53e-11	2.11
s12	-0.491e-11	12.2
s13	-0.758e-11	6.81
s33	2.01e-11	0.68
s44	4.49e-11	0.3
d15	7.21e-10	0.32
d13	-2.63e-10	-9.08
d33	6.521e-10	7.79

As part of a joint project with the Optimization Technology Center, run by Nortwestern University and the Argonne National Laboratory, we are testing a new approach for solving large scale optimization problems over the Internet.

This is an extension of the successful NEOS Server concept for the case in which large, private, commercial codes are necessary to calculate functions and derivatives associated with an optimization task. The assumption is that there is value in using the remote optimization facility, either because of consulting support or the use of proprietory optimization codes, or a combination of such facts. We have several problem areas in which such approach could be valuable, and chose this application as the first test.

The code we are using is J. Nocedal's LBFGS, a general optimization program with bound constraints. The code is activated from our local machine in California. By using several communication libraries provided by iNEOS, a channel is stablished through our firewall that connects with the iNEOS server in Illinois and starts the optimization code.

After that, a dialogue between these two processes is in effect: the iNEOS server requests various actions from our code, mainly the calculation of the Residual Mean Square functional and its partial derivatives at given values of the parameters. This requires 11 PZFLEX solves, and thus it takes about 10' to respond. The fitted real and imaginary parts of the impedance are shown in Figures 5 and 6. See [7] for more details.

6. Conclusions

In the typical example above we have been able to recover half of the parameters to the desired accuracy, an additional parameter has been improved by more than 50%, while the estimates for the remaining parameters have been worsened. Observe that our bound constraints allow for a maximum error of 16% in the worst case scenario.

We also see that the fit of the Fourier Transform of the impedance data is quite adequate, specially for the low frequencies. From experience in fitting this type of data by trial and error, we conclude that this procedure is far superior, both in human time and accuracy.

References

1. *FLEX User's Manual*. (Weidlinger Associates, Los Altos, CA ,1998).
2. R.P. Brent, *Algorithms for Minimization Without Derivatives*, (Prentice Hall, New Jersey, 1973).
3. V. Pereyra, "Modeling, ray tracing, and block nonlinear travel-time inversion," *Pure and Applied Geophysics* 148, pp. 345-386 (1996).
4. N.N. Abboud, G.L. Wojcik, D.K. Vaughan, J. Mould, D.J. Powell, and L. Nikodym, "Finite element modeling for ultrasonic transducers," *Proc. SPIE Ist Symp. Medical Imaging,* 1998.
5. G.L. Wojcik, D.K. Vaughan, N.N. Abboud and J. Mould, "Electromechanical modeling using explicit time-domain finite elements," *IEEE Ultrasonics Symp. Proc.,* 1993.
6. D.L.B. Jupp and K. Vozoff, "Stable iterative methods for the inversion of geophysical data," *Geophys. J. R. astr. Soc.* 42, pp. 957-976 (1975).
7. M. Good, J.-P. Goux, J. Nocedal and V. Pereyra, "iNEOS: an interactive environment for nonlinear optimization," to appear (2000).

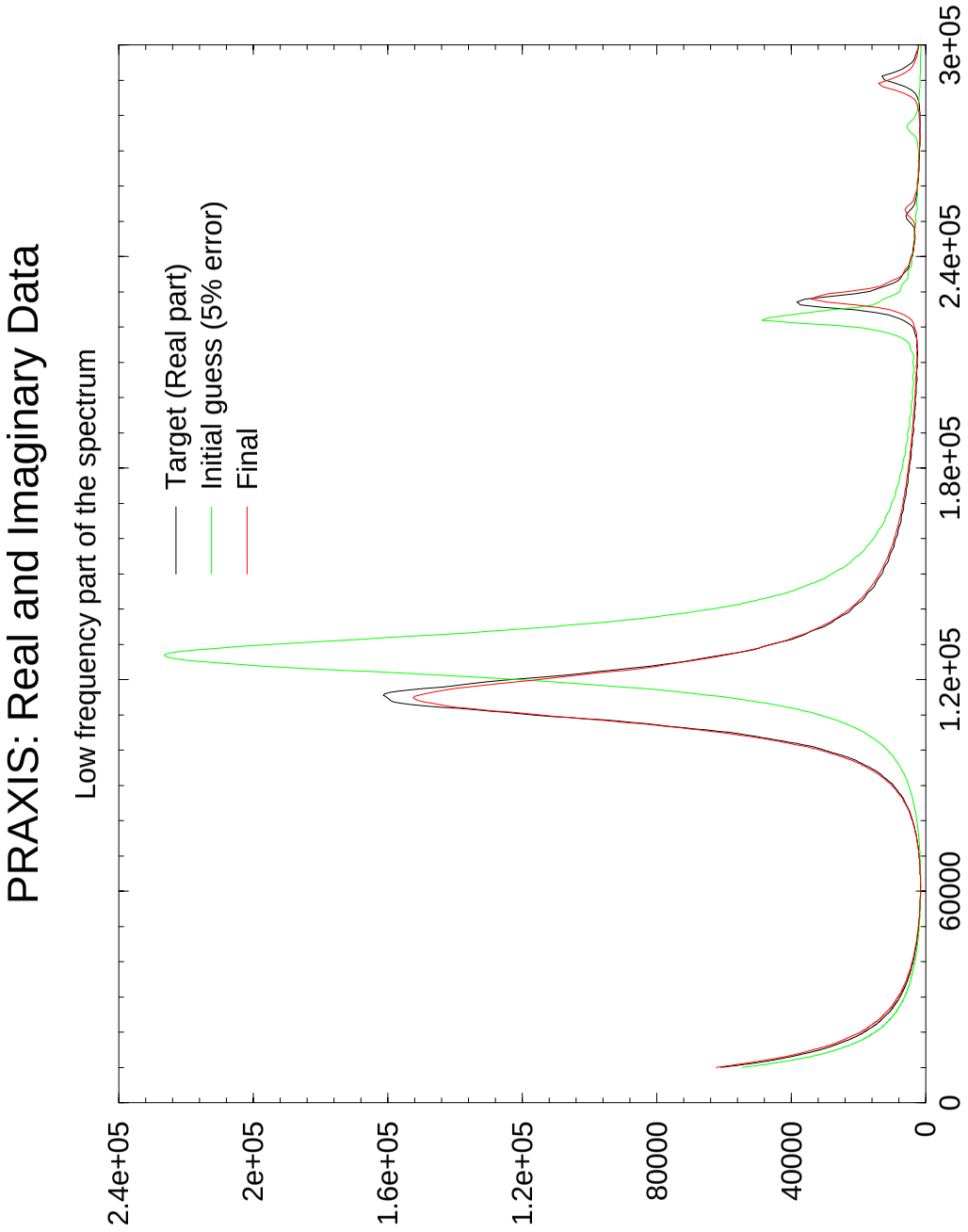
PRAXIS: Real and Imaginary Data
Low frequency part of the spectrum
Target (Real part)
Initial guess (5% error)
Final
2.4e+05
2e+05
1.6e+05
1.2e+05
80000
40000
0
0
60000
1.2e+05
1.8e+05
2.4e+05
3e+05

Figure 1:

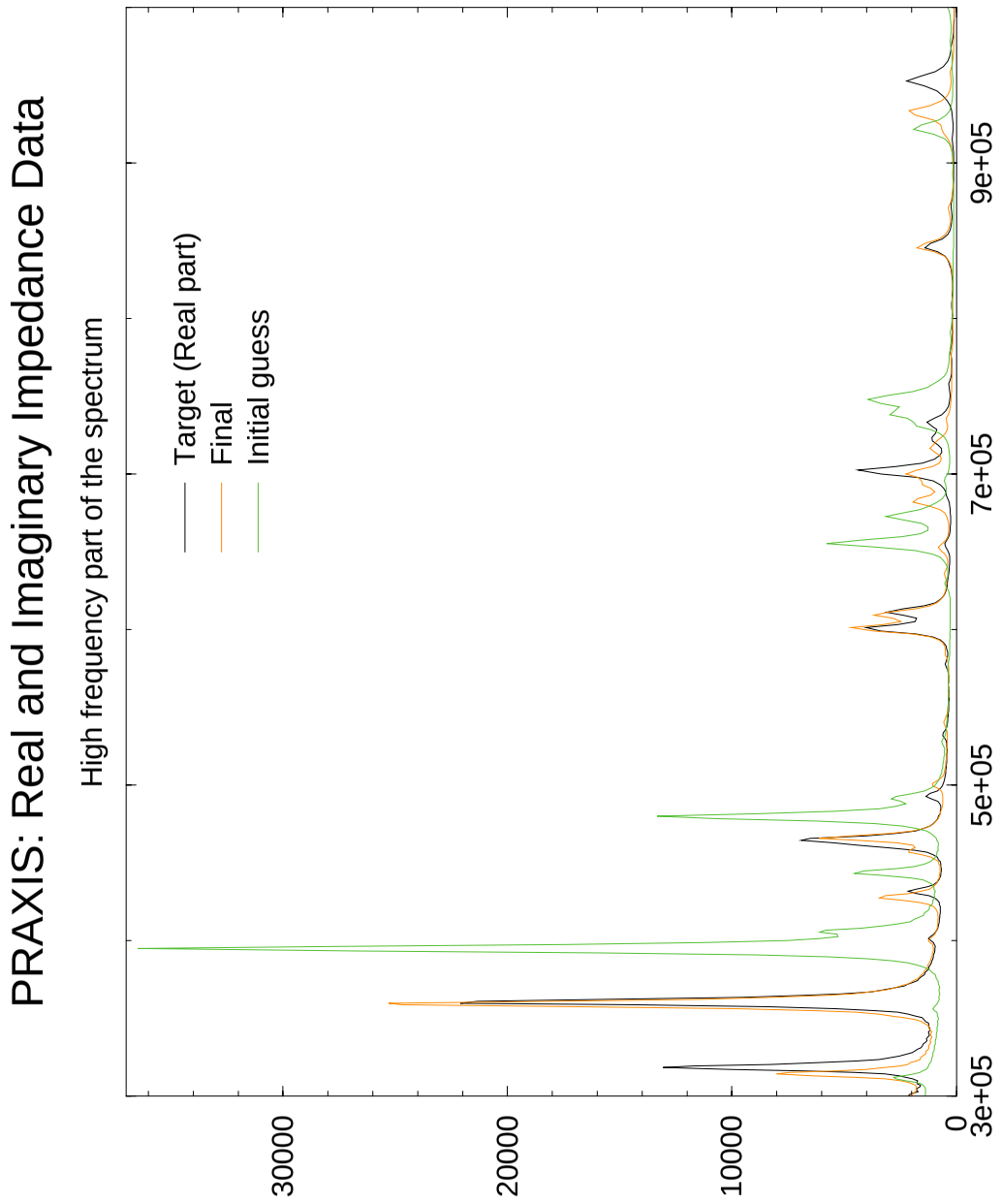
PRAXIS: Real and Imaginary Impedance Data
High frequency part of the spectrum
Target (Real part)
Final
Initial guess
30000
20000
10000
0
3e+05
5e+05
7e+05
9e+05

Figure 2:

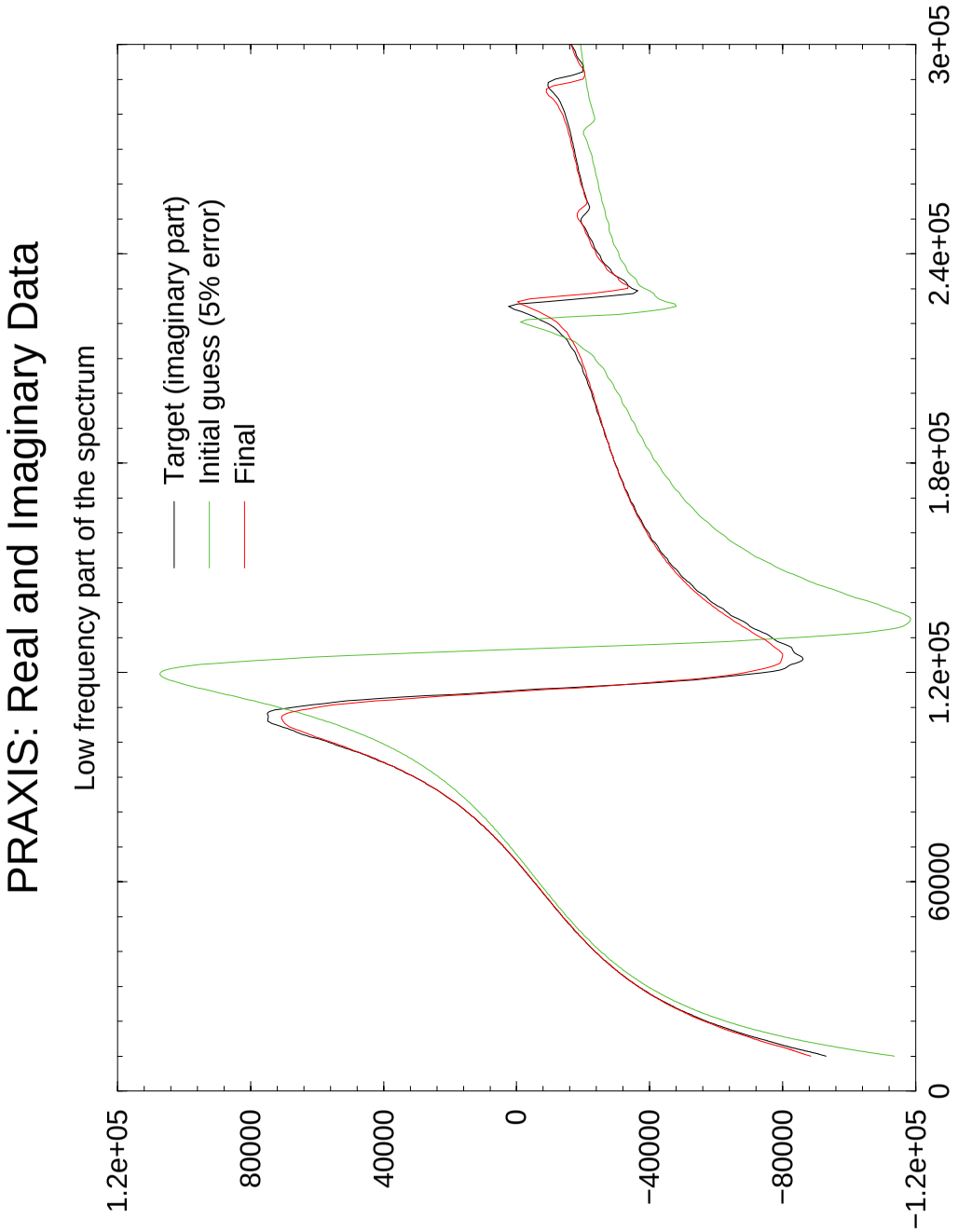
PRAXIS: Real and Imaginary Data
Low frequency part of the spectrum
Target (imaginary part)
Initial guess (5% error)
Final
1.2e+05
80000
40000
0
−40000
−80000
−1.2e+05
0
60000
1.2e+05
1.8e+05
2.4e+05
3e+05

Figure 3:

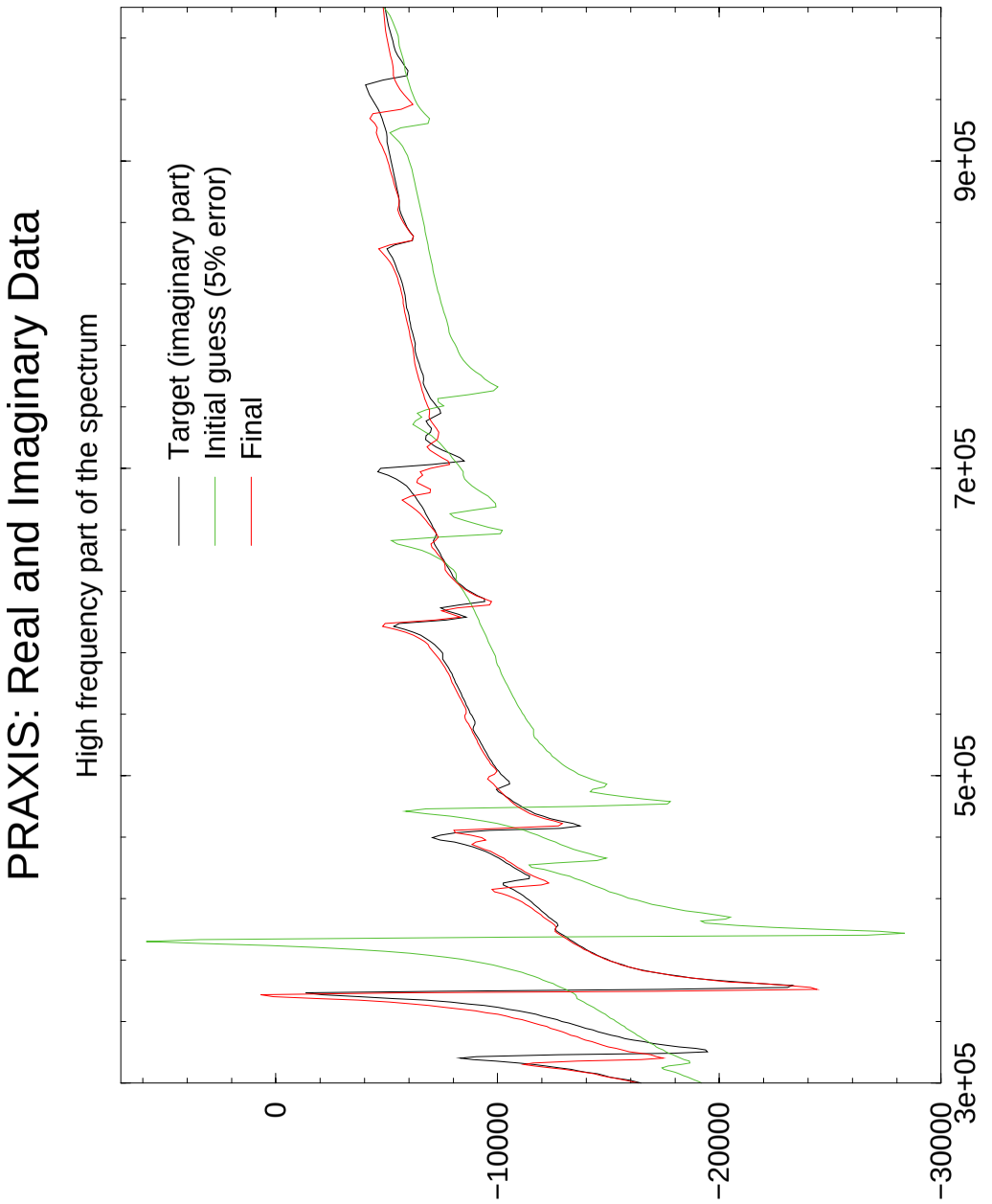
PRAXIS: Real and Imaginary Data
High frequency part of the spectrum
Target (imaginary part)
Initial guess (5% error)
Final
0
−10000
−20000
−30000
3e+05
5e+05
7e+05
9e+05

Figure 4:

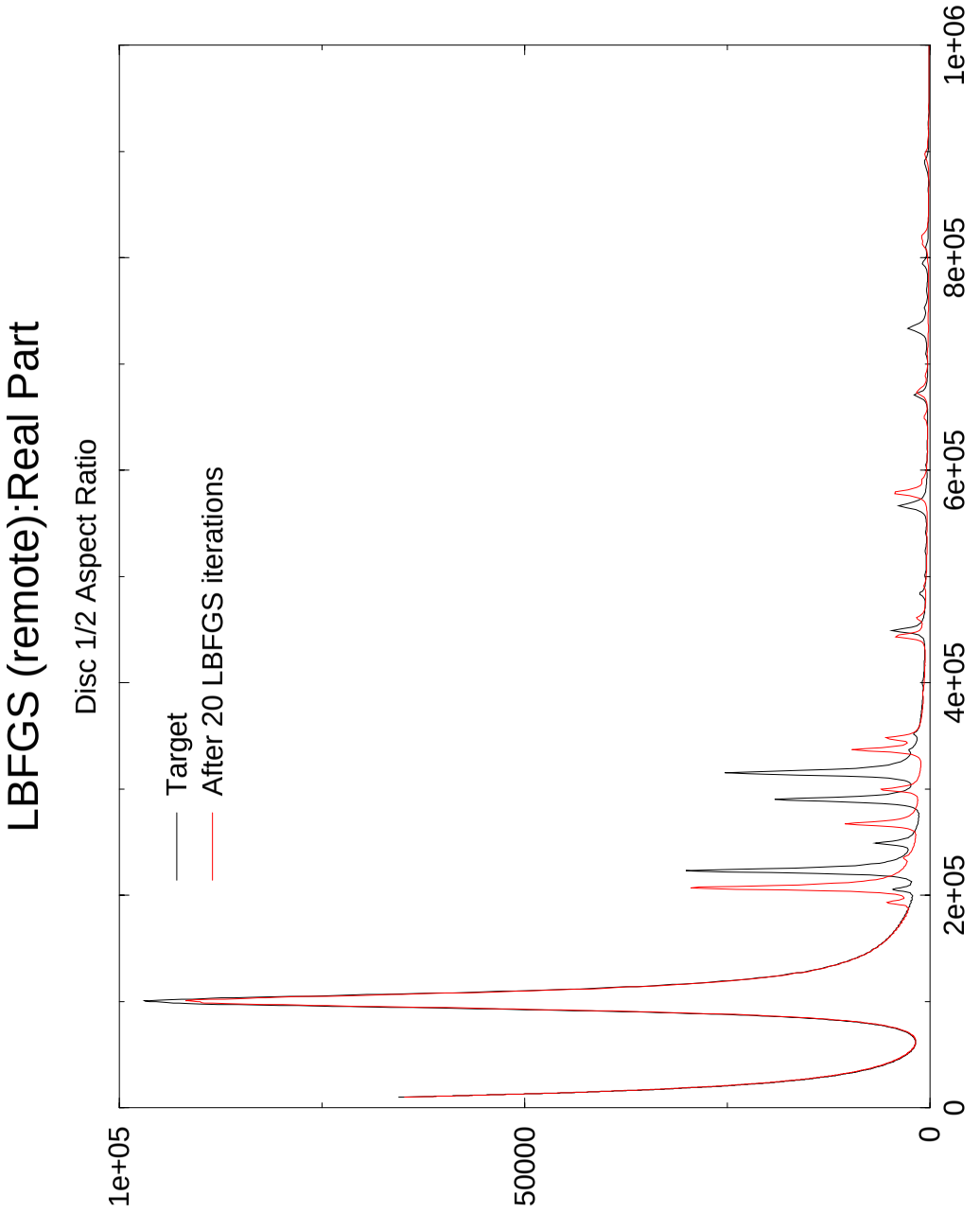
LBFGS (remote):Real Part
Disc 1/2 Aspect Ratio
Target
After 20 LBFGS iterations
1e+05
50000
0
0
2e+05
4e+05
6e+05
8e+05
1e+06

Figure 5:

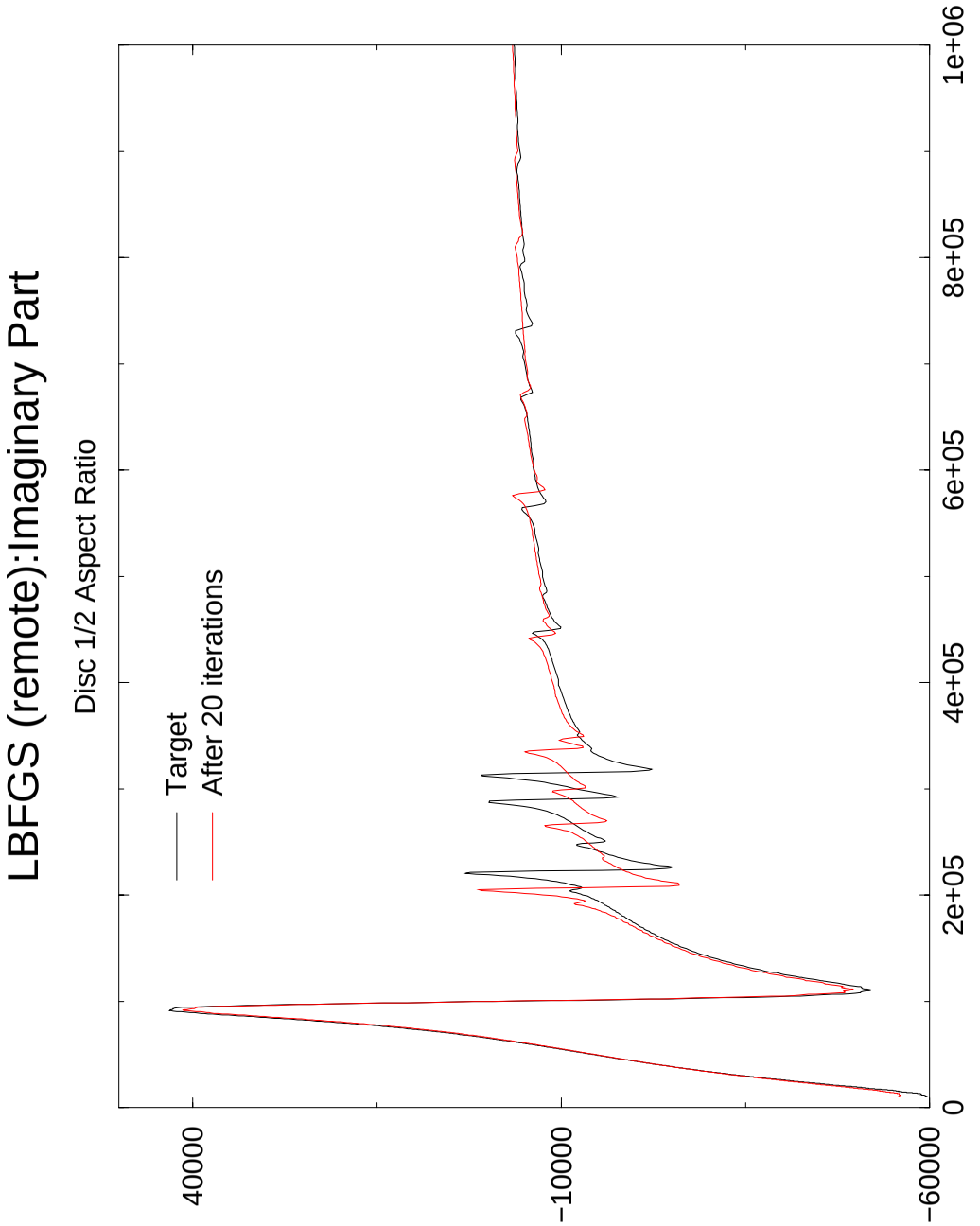
LBFGS (remote):Imaginary Part
Disc 1/2 Aspect Ratio
Target
After 20 iterations
40000
−10000
−60000
0
2e+05
4e+05
6e+05
8e+05
1e+06

Figure 6: